Dimensional crossover of the exchange-correlation energy at the semilocal level

Lucian A. Constantin
Department of Physics and Quantum Theory Group, Tulane University, New Orleans, Louisiana 70118, USA
(Received 23 June 2008; revised manuscript received 3 August 2008; published 7 October 2008)

Commonly used semilocal density-functional approximations for the exchange-correlation energy fail badly when the true two-dimensional limit is approached. We show, using a quasi-two-dimensional uniform electron gas in the infinite-barrier model, that the semilocal level can correctly recover the exchange-correlation energy of the two-dimensional uniform electron gas. We derive different, exact constraints at the semilocal level for the dimensional crossover of the exchange-correlation energy and we propose a method to incorporate them in any exchange-correlation density-functional approximation.

DOI: 10.1103/PhysRevB.78.155106 PACS number(s): 71.15.Mb, 71.45.Gm, 71.10.Ca

I. INTRODUCTION

In the Kohn-Sham (KS) time-independent density-functional theory the noninteracting kinetic energy is treated as an exact functional of the occupied orbitals[1] and only the exchange-correlation (xc) energy $E_{\rm xc}$ has to be approximated. The "Jacob's ladder" classification[2] of the ground-state density-functional approximations for $E_{\rm xc}$ has three complete nonempirical rungs: the local-spin-density approximation (LSDA),[1] the generalized gradient approximation (GGA),[3,4] and the meta GGA (MGGA).[5] Higher rungs of the ladder require new ingredients in order to satisfy more exact constraints.[2] Thus, the meta GGA has (as ingredients) the spin densities $n_\uparrow$ and $n_\downarrow$, their gradients $\nabla n_\uparrow$ and $\nabla n_\downarrow$, and the KS noninteracting kinetic-energy densities $\tau_\uparrow$ and $\tau_\downarrow$. The local and semilocal density functionals (LSDA, GGA, and meta GGA) give accurate predictions of ground state for atoms, molecules, solids,[6,7] and surfaces.[8] They also work for atomic monolayers[9,10] and other quasi-two-dimensional (quasi-2D) systems,[11] but they fail badly as the true 2D limit is approached.[12,13] The failure of the semilocal density functionals to describe the dimensional crossover of the exact xc functional can be avoided by using nonlocal models[14,15] such as the weighted density approximation,[16] or higher rungs of the Jacob's ladder.[17] Thus, the fourth-rung hyper GGA, a nonlocal correlation functional compatible with exact exchange,[18] improves considerably the behavior of semilocal functionals over the whole thickness range of the quasi-2D electron gas.[17] The numerically expensive fifth-rung approximations such as the inhomogeneous Singwi-Tosi-Land-Sjölander (ISTLS) method,[19] and the GW[20] approximation are remarkably accurate for the description of quasi-2D systems.[15,17]

The quasi-2D electron gas is experimentally realizable in silicon metal-oxide-semiconductor field-effect transistor and in the widely used semiconductor heterojunctions.[13,21] Other physical systems with strong 2D character are the copper-oxide planes of high-temperature superconductors and the electrons bound to the surface of liquid helium.[21]

This paper is organized as follows. In Sec. II, we present the exact constraints at the semilocal level for the dimensional crossover of the exchange-correlation energy. In Sec. III, we construct a simple semilocal functional that incorporates these exact conditions, and we test it for the quasi-2D uniform electron gas, jellium slabs, and nonuniformly scaled hydrogen atom. In Sec. IV, we summarize our conclusions.

II. EXACT CONDITIONS FOR SEMILOCAL DENSITY FUNCTIONALS

A 2D uniform electron gas is described by the 2D electron-density parameter $r_s^{\rm 2D}=1/\sqrt{\pi n^{\rm 2D}}=\sqrt{2}/k_F^{\rm 2D}$. (Unless otherwise stated, atomic units are used throughout, i.e., $e^2=\hbar=m_e=1$.) Here $n^{\rm 2D}$ is the density of electrons per unit area and $k_F^{\rm 2D}$ represents the magnitude of the corresponding 2D Fermi wave vector. The exchange energy per particle of the 2D uniform electron gas is[22]

$$\epsilon_x^{\rm 2D}=-[4\sqrt{2}/(3\pi)]/r_s^{\rm 2D}=-0.6002/r_s^{\rm 2D}. \quad (1)$$

The correlation energy per particle of a 2D uniform electron gas in the high-density limit ($r_s^{\rm 2D}\to 0$) is[22]

$$\epsilon_c^{\rm 2D}=-0.19-0.086r_s^{\rm 2D}\ln r_s^{\rm 2D}+O(r_s^{\rm 2D}), \quad (2)$$

and in the low-density limit ($r_s^{\rm 2D}\to\infty$), it is[22]

$$\epsilon_c^{\rm 2D}=\left(\frac{8}{3\pi}-2+\frac{4\sqrt{2}}{3\pi}\right)(r_s^{\rm 2D})^{-1}+(r_s^{\rm 2D})^{-3/2}+O[(r_s^{\rm 2D})^{-2}]. \quad (3)$$

A realistic interpolation (which uses quantum Monte Carlo data) between the high- and low-density limits of the 2D correlation energy per electron has the following form:[12,22]

$$\epsilon_c^{\rm 2D}=0.5058\left[\frac{1.3311}{(r_s^{\rm 2D})^2}(\sqrt{1+1.5026r_s^{\rm 2D}}-1)-\frac{1}{r_s^{\rm 2D}}\right]. \quad (4)$$

Similarly to Ref. 17, let us consider a quantum well of thickness L in the z direction. In the infinite-barrier model (IBM) (Ref. 23) for a quantum well, the KS effective one-electron potential is zero inside the well and infinity outside it, such that the KS orbital is

$$\Psi_{l,k}=\sqrt{\frac{2}{AL}}\sin\left(\frac{l\pi z}{L}\right)e^{i\mathbf{r}_\parallel\mathbf{k}_\parallel}\ \text{for}\ 0\le z\le L,\quad l\ge 1, \quad (5)$$

where A is the area of the xy plane, l is the subband index, and $\mathbf{r}_\parallel$ and $\mathbf{k}_\parallel$ are the position and the wave vector parallel to the surface. In this model the electrons cannot leak out of the

well, so the true 2D electron-gas limit is recovered by shrinking the well. The energy levels of this model are[12]

$$E_{l,k} = \frac{1}{2}\left[\left(\frac{l\pi}{L}\right)^2 + k_{\parallel}^2\right]. \quad (6)$$

When only the lowest level is occupied [$E_{1,k_F^{2D}} < E_{2,0}$, which implies $L < \sqrt{3/2}\pi r_s^{2D} = L_{max}$ (Ref. 12)], the density of states of this system begins to resemble the density of states of a 2D electron gas, the motion in the z direction is frozen out, and the system can be considered quasi-two-dimensional.

By shrinking the z coordinate without changing the total number of electrons per unit area, the system reaches the 2D electron-gas limit. This process is equivalent to a nonuniform scaling in one dimension,[24] and the three-dimensional (3D) scaled density is[12]

$$n_\lambda^z(z) = \frac{2}{(L/\lambda)\pi(r_s^{2D})^2}\sin^2\left(\frac{\pi z}{(L/\lambda)}\right); \quad 0 \le z \le L/\lambda, \quad (7)$$

where $n_\lambda^z(x,y,z) = \lambda n(x,y,\lambda z)$ and λ is the scaling parameter. When $\lambda \to \infty$, $L/\lambda \ll L_{max}$, and the 2D limit is achieved. The corresponding exchange and correlation energies per particle should satisfy the following scaling relations:[12]

$$\lim_{\lambda\to\infty}\frac{1}{N}E_x[n_\lambda^x] > -\infty; \quad \lim_{\lambda\to\infty}\frac{1}{N}E_c[n_\lambda^x] > -\infty, \quad (8)$$

where $N = \int_0^L n(z)dz$. These equations, which started from those of Ref. 24, are not satisfied by LSDA, GGA, or meta GGA.

The GGA exchange-correlation energy per particle of our quantum well of thickness L is

$$\frac{E_{xc}^{GGA}}{N} = \left\{\int_0^L n(z)\epsilon_{xc}^{GGA}[n(z),\nabla n(z)]dz\right\}/N, \quad (9)$$

and the meta-GGA exchange-correlation energy per particle is

$$\frac{E_{xc}^{MGGA}}{N} = \left\{\int_0^L n(z)\epsilon_{xc}^{MGGA}[n(z),\nabla n(z),\tau(z)]dz\right\}/N, \quad (10)$$

where ϵ_{xc}^{GGA} and ϵ_{xc}^{MGGA} are the GGA and meta-GGA xc energies per particle of the 3D system.

The positive kinetic-energy density of the IBM quasi-2D electron gas is

$$\tau = \tau^W + \frac{(k_F^{2D})^4}{4\pi(L/\lambda)}\sin^2\left(\frac{\pi z}{(L/\lambda)}\right) \ge \tau^W, \quad (11)$$

where $\tau^W = \pi(k_F^{2D})^2/[2(L/\lambda)^3]\cos^2[\frac{\pi z}{(L/\lambda)}]$ is the von Weizsäcker kinetic-energy density.[25] When $\lambda \to \infty$, $\tau \to \tau^W \sim \lambda^3$ and $\tau - \tau^W \sim \lambda$. Equation (11) can be well described by the Laplacian-level meta-GGA kinetic-energy density of Ref. 26.

The reduced gradients for exchange $\{p = |\nabla n|^2/[4(3\pi^2)^{2/3}n^{8/3}] \sim \lambda^{4/3}\}$ measure the variation in the density over a Fermi wavelength, and that for correlation $\{t = |\nabla n|/[4(3/\pi)^{1/6}n^{7/6}] \sim \lambda^{5/6}\}$ measures the variation in the density over the screening length. Both tend to infinity when the 2D limit is reached ($\lambda \to \infty$) such that in the quasi-2D electron-gas regime, the density is rapidly varying almost everywhere. Thus this system is not only a challenge for a semilocal density functional but it can also give exact constraints (at the semilocal level) in the regime where the 3D density and its gradient diverge.

The exact exchange energy per particle of the 2D uniform electron gas [see Eq. (1)] can be *correctly* recovered by any 3D semilocal density-functional approximation for exchange energy if in the large-gradient limit ($p \to \infty$), the 3D exchange energy per particle behaves as $a_x p^{-1/4}\epsilon_x^{LSDA}$ (see Ref. 27), where

$$a_x = (0.6002\sqrt{2}\pi)/\left[3^{3/2}\int_0^1 dy\, \sin^{7/2}(\pi y)\cos^{-1/2}(\pi y)\right] \quad (12)$$

was derived in the IBM model using Eqs. (1) and (9). Equation (12) gives $a_x = 0.5217$. The parameter a_x (as well as the other results of this section), even if calculated using the IBM quasi-2D electron gas, is independent of the quantum-well potential model along the confinement z direction because the 2D limit ($\lambda \to \infty$) is not relaying on the effective potential model.

At a meta-GGA level, we can also use the dimensionless inhomogeneity parameter[5,28]

$$\alpha = \frac{\tau - \tau^W}{\tau^{unif}} \sim \lambda^{-2/3}, \quad (13)$$

where $\tau^{unif} = (3/10)(3\pi^2)^{2/3}n^{5/3}$ is the Thomas-Fermi kinetic-energy density of the 3D uniform electron gas.[29] Thus Eq. (1) can also be *exactly* satisfied by any meta GGA if in the large-gradient limit ($p \to \infty$), the 3D exchange energy per particle behaves as $b_x\alpha^{1/2}\epsilon_x^{LSDA}$, where $b_x = 1.947$ was found similarly as a_x from Eqs. (1) and (10).

Because r_s^{2D} enters in a nonlinear manner in Eq. (4), the GGA level cannot describe the correlation energy per particle of a 2D uniform electron gas, but it can explain the 2D high- and low-density limits. The high-density limit of Eq. (2) can be exactly recovered by any 3D GGA that behaves in the large-gradient limit ($t \to \infty$) as

$$\epsilon_c^{GGA} \to -0.19 - 0.0497n^{-5/12}\sqrt{t}\,\ln(n^{-5/12}\sqrt{t}), \quad (14)$$

where $t \sim \lambda^{5/6}$ is the reduced gradient for correlation. The low-density limit of Eq. (3) can also be exactly recovered by any 3D GGA that behaves in the large-gradient limit ($t \to \infty$) as

$$\epsilon_c^{GGA} \to -0.403\,45n^{5/12}t^{-1/2} + 0.459n^{5/8}t^{-3/4}. \quad (15)$$

At the meta-GGA level, Eq. (4) can be correctly satisfied by any 3D meta GGA that behaves in the large-gradient limit ($t \to \infty$) as

$$\epsilon_c^{MGGA} \to \epsilon_c^{2D}, \quad (16)$$

where ϵ_c^{2D} is given by Eq. (4) and

$$r_s^{2D} = 0.4173 n^{-1/3} \alpha^{-1/2} = 0.6727 r_s^{3D} \alpha^{-1/2}. \quad (17)$$

Equation (17) connects r_s^{2D} with r_s^{3D} showing the importance of the α ingredient to the dimensional crossover of the exchange-correlation energy and to the nonuniform scaling in one dimension.

III. CONSTRUCTION AND TESTS OF A SIMPLE SEMILOCAL FUNCTIONAL

The results of Sec. II can be included in any density-functional approximation for the exchange-correlation energy. For simplicity, we incorporate them in the LSDA. Let us consider first the exchange part and define GGA+2D and MGGA+2D as

$$\epsilon_x^{GGA+2D} = \epsilon_x^{LSDA}\{1 + f(p)[-1 + 0.5217 p^{-1/4}]\} \quad (18)$$

and

$$\epsilon_x^{MGGA+2D} = \epsilon_x^{LSDA}\{1 + f(p)[-1 + 1.947 \alpha^{1/2}]\}, \quad (19)$$

where $f(p)=1$ for $p=\infty$. The simplest approximation for $f(p)$ is a step function

$$f(p) = \lim_{x\to\infty} \theta(p - x), \quad (20)$$

where $\theta(x)$ is 0 for $x<0$ and 1 for $x \geq 0$. This model preserves all the exact constraints that the local or semilocal functional satisfies and recovers the exchange energy of the 2D uniform electron gas in the limit $L=0$ (when $p=\infty$). However, this approximation does not improve the behavior of the semilocal functional in the quasi-2D region, and moreover, it gives a discontinuity when $p \to \infty$.

We propose the following simple analytic model for the function $f(p)$ (Ref. 30):

$$f(p) = \frac{p^4(1+p^2)}{10^c + p^6}, \quad (21)$$

where $c>0$ is an empirical parameter. Equation (21) recovers the right limit when $p \to \infty$ [$f(p \to \infty)=1$], and for a slowly varying density, when p is small ($p<1$), it behaves as $f(p) \sim [p^4 1 \times 10^{-c} + \text{higher-order terms}]$. This is a good feature because it can accurately preserve the behavior of the semilocal functional in the slowly varying limit.[31] When c is large, Eq. (21) starts to model Eq. (20).

In Fig. 1, we show the exchange energy per particle of the quasi-2D electron gas with 2D bulk parameter $r_s^{2D}=4$ for several density functionals: exact exchange, LSDA, PBE[3] GGA, GGA+2D of Eq. (18), and MGGA+2D of Eq. (19), using in Eq. (21) three values for the parameter c ($c=2$, 8, and 16). LSDA and PBE diverge when $L \to 0$ ($\lambda \to \infty$). The meta-GGA TPSS,[5] not plotted in Fig. 1, has the same behavior as PBE. Both GGA+2D and MGGA+2D perform better than LSDA at small thicknesses of the quantum well, and both of them recover the exact exchange energy of the 2D uniform electron gas when $L=0$. However, we observe that GGA+2D with $c=2$ [the curve denoted by (GGA+2D)(a)] is the most accurate and remarkably describes the quasi-2D region. When the value of parameter c increases, the GGA

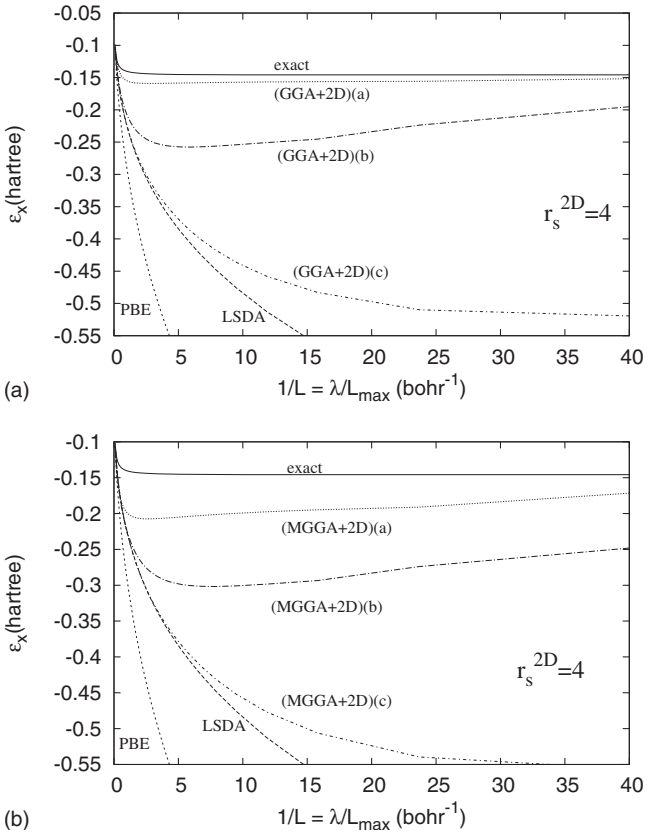

FIG. 1. Exchange energy per particle of an IBM quasi-2D electron gas of fixed 2D electron density ($r_s^{2D}=4$) as a function of the inverse quantum well thickness $1/L$ ($L<L_{max}=15.39$). The curves denoted by (GGA+2D)(a), (GGA+2D)(b), and (GGA+2D)(c) are those given by Eq. (18) using for $f(p)$ the analytic model of Eq. (21) with $c=2$, 8, and 16, respectively. The curves denoted by (MGGA+2D)(a), (MGGA+2D)(b), and (MGGA+2D)(c) are those given by Eq. (19) using for $f(p)$ the analytic model of Eq. (21) with $c=2$, 8, and 16, respectively. While the LSDA and PBE diverge, all GGA+2D and MGGA+2D curves recover in the limit $\lambda \to \infty$ [the corresponding exchange energy (−0.150 05) of a 2D electron gas].

+2D and MGGA+2D have the LSDA behavior over a larger region, and consequently, they are not accurate in the quasi-2D region. We also remark that GGA+2D and MGGA+2D calculated with $c=8$ [the curves (GGA+2D)(b) and (MGGA+2D)(b)] give a significant improvement over the LSDA in the whole quasi-2D region.

In Fig. 2, we show the exchange energy per particle of a thick jellium slab of bulk parameter $r_s^{3D}=2.07$. [The bulk parameter defined by the equation $n=3/4\pi(r_s^{3D})^3$ represents the radius of a sphere that encloses on average one electron.] The local and semilocal density approximations (LSDA, TPSS, GGA+2D, and MGGA+2D) show an exponential decay of the exchange energy per particle whereas the exact exchange behaves as $\approx -1/(4z)$.[32] All the MGGA+2D curves have a bump in the region where $f(p)$ switches from 0 to 1, and after that they are close to the TPSS meta-GGA exchange energy per particle. (We recall that TPSS meta GGA has the same large-p behavior as the PBE GGA.) We observe that for jellium slabs (as well as for many 3D sys-

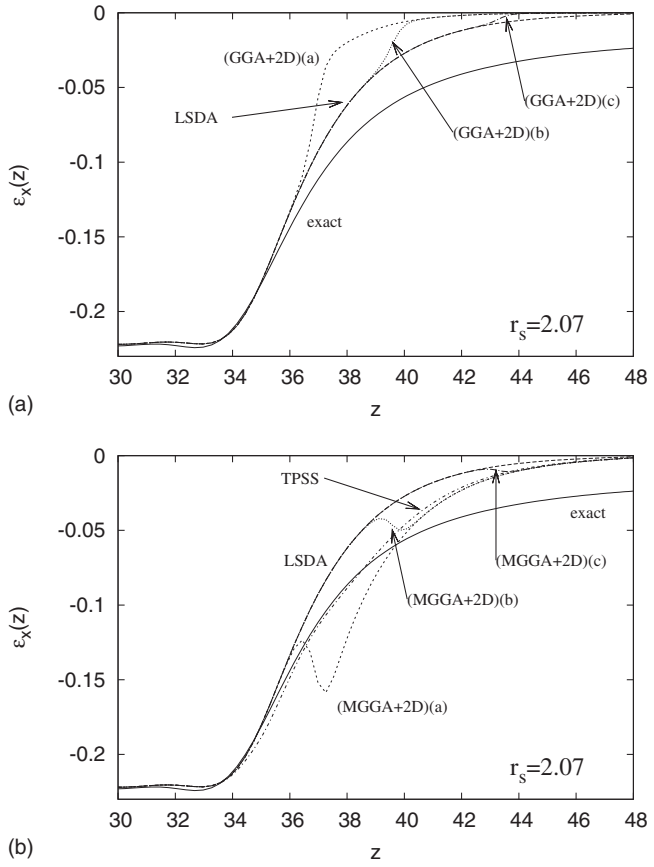

FIG. 2. Exchange energy per particle at position z versus z in atomic units at a jellium-slab surface. The bulk parameter is $r_s^{3D}=2.07$, the slab width is $d=3.2\lambda_F$, and the jellium surface is at $z=35.24$ a.u. ($\lambda_F=2\pi/k_F^{3D}$ is the Fermi wavelength). The calculations of the exact exchange, LSDA, TPSS, GGA+2D, and MGGA+2D use the LSDA Kohn-Sham orbitals. The curves (GGA+2D)(a), (GGA+2D)(b), (GGA+2D)(c), (MGGA+2D)(a), (MGGA+2D)(b), and (MGGA+2D)(c) have the same signification as in Fig. 1.

tems) $E_x^{\mathrm{GGA+2D}}>E_x^{\mathrm{LSDA}}$, whereas $E_x^{\mathrm{MGGA+2D}}<E_x^{\mathrm{LSDA}}$, thus one can try also a convex combination between Eqs. (18) and (19). However, the construction of an accurate 3D and quasi-2D semilocal functionals is a difficult task[33,34] and is beyond the purpose of this paper.

Since p values bigger than 9 are found in the tail of an atom or molecule, where the electron density is negligible, we can choose $c=8$ (such that at $p=9$, $f=0.0053$ and for $p>50$, $f\to 1$). This choice ensures that the GGA+2D of Eq. (18) and MGGA+2D of Eq. (19) perform similarly with LSDA for 3D systems, make a considerable improvement in quasi-2D region, and recover the exchange energy of the 2D uniform electron gas. Thus, from now, all the presented calculations use $c=8$ in Eq. (21).

Similar with the exchange case, the correlation results of Sec. II can be included in any density-functional approximation; however, for simplicity we again show them for the LSDA case. Thus, we define

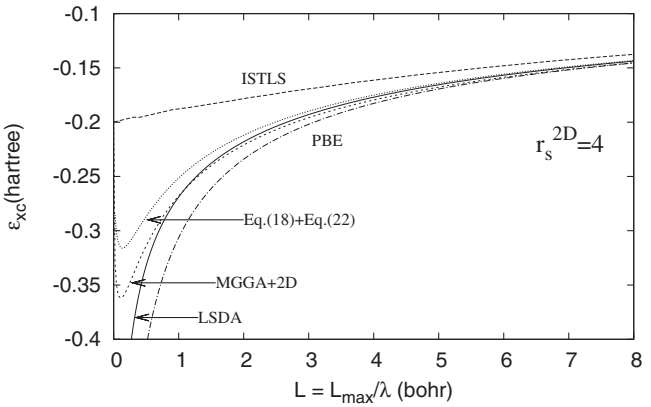

FIG. 3. Exchange-correlation energy per particle of an IBM quasi-2D electron gas of fixed 2D electron density ($r_s^{2D}=4$) as a function of the quantum well thickness L ($L<L_{\max}=15.39$). While LSDA and PBE diverge in the 2D limit, MGGA+2D and $\epsilon_x^{\mathrm{GGA+2D}}+\epsilon_c^{\mathrm{GGA+2D}}$ [see Eqs. (18) and (22)] approach the exact 2D limit.

$$\epsilon_c^{\mathrm{MGGA+2D}}=\epsilon_c^{\mathrm{LSDA}}+f(t)[-\epsilon_c^{\mathrm{LSDA}}+\epsilon_c^{\mathrm{2D}}], \tag{22}$$

where t is the reduced gradient for correlation, $f(t)$ has the same form as Eq. (21) (with $c=8$), and ϵ_c^{2D} is given by Eqs. (4) and (17).

Figures 3 and 4 show several approximations of the xc energy per particle versus the quantum-well thickness L for quasi-2D electron gases of fixed 2D electron-density parameters: $r_s^{2D}=4$ and $2/\sqrt{3}$ (as in Figs. 1 and 2 of Ref. 17). The ISTLS method,[19] a self-consistent approach that depends on all occupied and unoccupied KS orbitals, is remarkably accurate for any thickness $L=L_{\max}/\lambda$ (see Ref. 17). LSDA and PBE are accurate in the limit $L\to L_{\max}$, but they fail badly in the zero-thickness limit. MGGA+2D and the xc energy per particle of Eqs. (18) and (22) ($\epsilon_x^{\mathrm{GGA+2D}}+\epsilon_c^{\mathrm{MGGA+2D}}$) are accurate in the limit $L\to L_{\max}$ and improve considerably the behavior of LSDA when $L<\sim 0.5L_{\max}$, approaching the exact 2D limit when $L\to 0$.

Let us present our results for the nonuniformly scaled hydrogen atom,[26,35] whose density is $n_\lambda(\mathrm{r})=(\lambda/\pi)\exp[-2\sqrt{x^2+y^2+(\lambda z)^2}]$. The exact xc energy is[35]

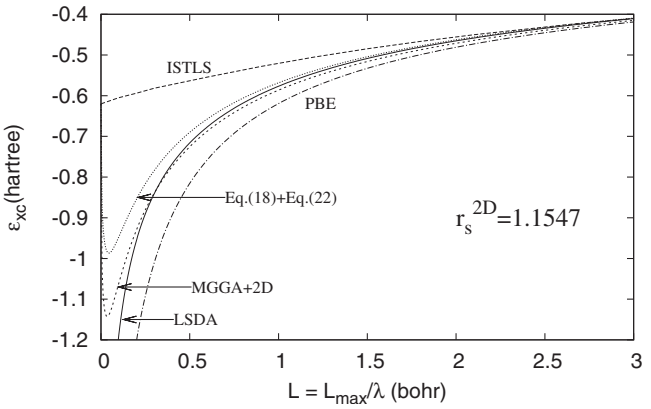

FIG. 4. As in Fig. 3 but now for $r_s^{2D}=2/\sqrt{3}$ ($L_{\max}=4.44$).

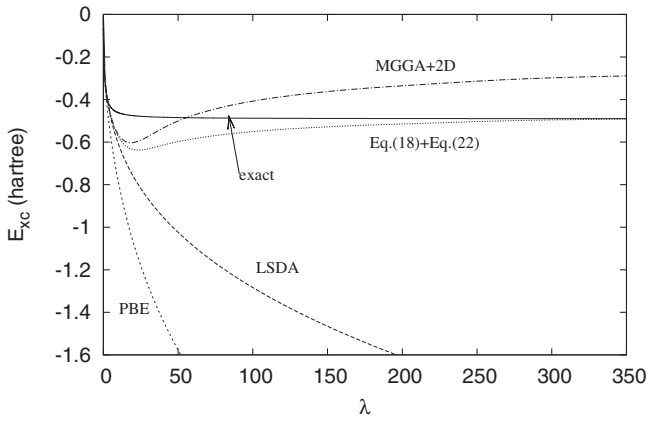

FIG. 5. Exchange-correlation energy versus scaling parameter λ for the nonuniformly scaled hydrogen atom. Also shown is the exact xc energy [see Eq. (23)].

$$E_{\mathrm{xc}}(\lambda)=\begin{cases}-\dfrac{5}{16}\dfrac{\lambda}{\sqrt{\lambda^2-1}}\arctan(\sqrt{\lambda^2-1}), & \lambda>1\\ -\dfrac{5}{16}, & \lambda=1\\ -\dfrac{5}{16}\dfrac{\lambda}{\sqrt{1-\lambda^2}}\ln\left(\dfrac{\sqrt{1-\lambda^2}+1}{\lambda}\right), & \lambda<1.\end{cases} \tag{23}$$

When $\lambda\to\infty$, this system can model an electron firmly bound to a surface. Figure 5 shows that LSDA and PBE fail badly in the extreme oblate case ($\lambda\gg 1$). The meta-GGA TPSS,[5] not plotted in Fig. 5, has the same behavior as PBE. Because in any one-electron system $\tau=\tau^W$ and $\alpha=0$, the MGGA +2D xc energy will slowly approach zero in the limit $\lambda\to\infty$. The xc energy of Eqs. (18) and (22) ($E_x^{\mathrm{GGA+2D}}+E_c^{\mathrm{MGGA+2D}}$) is very accurate at large values of λ.

In this section we have proposed a method that incorporates the 2D limit of the electron gas in semilocal functionals and keeps as much as possible the 3D accuracy of the semilocal functionals. However, in order to obtain a good description of the quasi-2D region, the empirical parameter c has to be smaller ($c\approx 2$) than the optimized value ($c=8$), but such a choice will significantly modify the 3D accuracy of the semilocal functional. In the investigation of physical systems with strong 2D character, Eq. (17) can be seen as an indicator of the quasi-2D electron-gas regime. Various indicators of the electron localization have been constructed for 3D systems (see for example Ref. 36), but Eq. (17) is a better and natural choice in the case of quasi-2D uniform gas. Thus, in the quasi-2D regions, where $r_s^{3D}(z)\alpha^{-1/2}(z)$ is constant, we can choose $c=2$ and in the other regions we can choose $c=8$ (or even $c=\infty$). Such a parametrization of c can be more useful in applications than the use of our optimized value for c ($c=8$).

IV. CONCLUSIONS

In summary, we have shown that the dimensional crossover (from 3D to 2D) of the exact xc energy can be significantly improved at a meta-GGA level, and we derive different exact constraints (see Sec. II) using an IBM quasi-2D electron gas. Same results can be obtained using the parabolic quantum well of Ref. 13 because the 2D limit is independent on the quasi-2D electron-gas model. Thus, a 3D meta GGA that requires input from the 3D uniform electron gas[37] can describe a 2D system using only the highly nonlocal region where $|\nabla n|\to\infty$. Moreover, Eq. (17) shows a close connection between r_s^{2D} and r_s^{3D} and the positive noninteracting kinetic-energy density τ in the case of the quasi-2D electron gas.

We propose a simple approach to incorporate the dimensional crossover constraints in any local or semilocal density-functional approximation for the xc energy, and we present it in the case of LSDA. However, future work is needed to construct an accurate meta GGA that satisfies the dimensional crossover constraints.

The nonuniform scaling in one dimension is closely related to the quasi-2D electron gas. The nonuniformly scaled hydrogen atom in the oblate case ($\lambda\geq 1$), an important and hard test for the density functionals as well as a model for an electron bound to a surface, can be well described by our simple modified LSDAs. Thus we hope that this work can be useful not only for investigation of physical systems with strong 2D character, but also in developing more accurate density functionals.

ACKNOWLEDGMENTS

L.A.C. thanks John P. Perdew and J. M. Pitarke for many valuable discussions and suggestions. L.A.C. acknowledges support from NSF (Grant No. DMR05-01588).

[1] W. Kohn and L. J. Sham, Phys. Rev. **140**, A1133 (1965).
[2] J. P. Perdew and K. Schmidt, in *Density Functional Theory and its Applications to Materials*, edited by V. E. Van Doren, K. Van Alsenoy, and P. Geerlings (American Institute of Physics, Melville, NY, 2001).
[3] J. P. Perdew, K. Burke, and M. Ernzerhof, Phys. Rev. Lett. **77**, 3865 (1996).
[4] J. P. Perdew, A. Ruzsinszky, G. I. Csonka, O. A. Vydrov, G. E. Scuseria, L. A. Constantin, X. Zhou, and K. Burke, Phys. Rev. Lett. **100**, 136406 (2008).
[5] J. Tao, J. P. Perdew, V. N. Staroverov, and G. E. Scuseria, Phys. Rev. Lett. **91**, 146401 (2003).
[6] S. Kurth, J. P. Perdew, and P. Blaha, Int. J. Quantum Chem. **75**, 889 (1999).
[7] V. N. Staroverov, G. E. Scuseria, J. Tao, and J. P. Perdew, Phys. Rev. B **69**, 075102 (2004).
[8] L. A. Constantin, J. M. Pitarke, J. F. Dobson, A. Garcia-Lekue, and J. P. Perdew, Phys. Rev. Lett. **100**, 036401 (2008); J. M.

Pitarke, L. A. Constantin, and J. P. Perdew, Phys. Rev. B **74**, 045121 (2006); L. A. Constantin, J. P. Perdew, and J. Tao, *ibid.* **73**, 205104 (2006).
[9] K. Rytkönen, J. Akola, and M. Manninen, Phys. Rev. B **75**, 075401 (2007).
[10] M. C. Valero, P. Raybaud, and P. Sautet, Phys. Rev. B **75**, 045427 (2007).
[11] S. M. Reimann and M. Manninen, Rev. Mod. Phys. **74**, 1283 (2002).
[12] L. Pollack and J. P. Perdew, J. Phys.: Condens. Matter **12**, 1239 (2000).
[13] Y. H. Kim, I. H. Lee, S. Nagaraja, J. P. Leburton, R. Q. Hood, and R. M. Martin, Phys. Rev. B **61**, 5202 (2000).
[14] P. García-González, Phys. Rev. B **62**, 2321 (2000).
[15] P. García-González and R. W. Godby, Phys. Rev. Lett. **88**, 056406 (2002).
[16] O. Gunnarsson, M. Jonson, and B. I. Lundqvist, Phys. Rev. B **20**, 3136 (1979).
[17] L. A. Constantin, J. P. Perdew, and J. M. Pitarke, Phys. Rev. Lett. **101**, 016406 (2008).
[18] J. P. Perdew, V. N. Staroverov, J. Tao, and G. E. Scuseria, arXiv:0808.2523 (unpublished).
[19] J. F. Dobson, J. Wang, and T. Gould, Phys. Rev. B **66**, 081108(R) (2002).
[20] L. Hedin, Phys. Rev. **139**, A796 (1965).
[21] T. Ando, A. B. Fowler, and F. Stern, Rev. Mod. Phys. **54**, 437 (1982).
[22] M. Seidl, J. P. Perdew, and M. Levy, Phys. Rev. A **59**, 51 (1999), and references therein.
[23] D. M. Newns, Phys. Rev. B **1**, 3304 (1970).
[24] M. Levy and Hui Ou-Yang, Phys. Rev. A **42**, 651 (1990); Hui Ou-Yang and M. Levy, *ibid.* **42**, 155 (1990).
[25] C. F. von Weizsäcker, Z. Phys. **96**, 431 (1935).
[26] J. P. Perdew and L. A. Constantin, Phys. Rev. B **75**, 155109 (2007).
[27] This choice, found from the L-dependence of n and p, is necessary and sufficient that the exchange energy per particle of the quantum well [see Eq. (9)] to be finite (and nonzero) when $L=0$.
[28] J. P. Perdew, J. Tao, V. N. Staroverov, and G. E. Scuseria, J. Chem. Phys. **120**, 6898 (2004).
[29] L. H. Thomas, Proc. Cambridge Philos. Soc. **23**, 542 (1926); E. Fermi, Rend. Accad. Naz. Lincei **6**, 602 (1927).
[30] A smooth function that also interpolates between 0 and 1 was used in construction of the Laplacian-level meta-GGA kinetic energy density (see Fig. 1 of Ref. 26).
[31] For example, TPSS meta-GGA (Ref. 5) recovers the fourth-order gradient expansion for a slowly varying density.
[32] A. Solomatin and V. Sahni, Phys. Rev. B **56**, 3655 (1997).
[33] The satisfaction of Lieb-Oxford bound (Ref. 34) that is an important constraint in construction of accurate density functionals, is a challenge for a GGA+2D whose enhancement factor tends to zero when p becomes large.
[34] E. H. Lieb and S. Oxford, Int. J. Quantum Chem. **19**, 427 (1981).
[35] S. Kurth, J. Mol. Struct.: THEOCHEM **501-502**, 189 (2000).
[36] J. Tao, G. Vignale, and I. V. Tokatly, Phys. Rev. Lett. **100**, 206405 (2008).
[37] J. P. Perdew and Y. Wang, Phys. Rev. B **45**, 13244 (1992).